Translational Oncology 13 (2020) 100823

Contents lists available at ScienceDirect

Translational Oncology

journal homepage: www.elsevier.com/locate/tranon

Original research

CpG-coated Prussian blue nanoparticles-based photothermal therapy combined with anti-CTLA-4 immune checkpoint blockade triggers a robust abscopal effect against neuroblastoma

Juliana Cano-Mejia [a,b], Anshi Shukla [a], Debbie K. Ledezma [b,c], Erica Palmer [a], Alejandro Villagra [a], Rohan Fernandes [a,c,d,*]

[a] The George Washington Cancer Center, The George Washington University, Washington, DC 20052, USA
[b] Fischell Department of Bioengineering, University of Maryland, College Park, MD 20742, USA
[c] The Institute for Biomedical Sciences, The George Washington University, Washington, DC 20037, USA
[d] Department of Medicine, The George Washington University, Washington, DC 20037, USA

ARTICLE INFO

Article history:
Received 2 April 2020
Received in revised form 21 May 2020
Accepted 26 May 2020
Available online xxxx

Keywords:
Neuroblastoma
Prussian blue nanoparticles-based photothermal therapy
CpG oligodeoxynucleotides
Immune checkpoint blockade
Abscopal effect
Nanoimmunotherapy

ABSTRACT

High-risk neuroblastoma, which is associated with regional and systemic metastasis, is a leading cause of cancer-related mortality in children. Responding to this need for novel therapies for high-risk patients, we have developed a "nanoimmunotherapy," which combines photothermal therapy (PTT) using CpG oligodeoxynucleotide-coated Prussian blue nanoparticles (CpG-PBNPs) combined with anti-CTLA-4 (aCTLA-4) immunotherapy. Our *in vitro* studies demonstrate that in addition to causing ablative tumor cell death, our nanoimmunotherapy alters the surface levels of co-stimulatory, antigen-presenting, and co-inhibitory molecules on neuroblastoma tumor cells. When administered in a syngeneic, murine model of neuroblastoma bearing synchronous Neuro2a tumors, the CpG-PBNP-PTT plus aCTLA-4 nanoimmunotherapy elicits complete tumor regression in both primary (CpG-PBNP-PTT-treated) and secondary tumors, and long-term survival in a significantly higher proportion (55.5%) of treated-mice compared with the controls. Furthermore, the surviving, nanoimmunotherapy-treated animals reject Neuro2a rechallenge, suggesting that the therapy generates immunological memory. Additionally, the depletion of $CD4^+$, $CD8^+$, and NK^+ populations abrogate the observed therapeutic responses of the nanoimmunotherapy. These findings demonstrate the importance of concurrent PTT-based cytotoxicity and the antitumor immune effects of PTT, CpG, and aCTLA-4 in generating a robust abscopal effect against neuroblastoma.

Introduction

Neuroblastoma is the most common extracranial solid tumor of childhood, accounting for 15% of cancer-related deaths in children [1,2]. A majority of high-risk neuroblastoma patients present with metastatic disease at diagnosis, which confers an increased risk of recurrence and a dismal prognosis, with overall survival rates ranging from 30 to 40% [3]. Current treatment modalities for this high-risk group, including high-dose chemotherapy, radiation, and surgery, have made incremental but limited progress because they result in incomplete tumor eradication and are ineffective in preventing relapse, and treating disseminated disease.

In response to the need for more effective therapies, we have designed an ensemble "nanoimmunotherapy" that combines state-of-the-art advances in the field of nanotechnology and immunotherapy for treating neuroblastoma. Specifically, we utilize nanoparticle-based photothermal therapy (PTT), which causes light-activated thermal ablation of tumors [4]. PTT also elicits antitumor immune responses [5–12], and increasing evidence suggests that localized photothermal killing of a primary tumor (*via* PTT) can induce immune-mediated regression in distant untreated tumors [5,13], a process termed as the abscopal effect [14–17]. While beneficial for treating disseminated cancer, the abscopal effects of PTT are often restricted by an immunosuppressive microenvironment within tumors [18]. Therefore, these effects have been rarely observed when administering PTT, and similarly with other locally ablative modalities alone, including hyperthermia or radiation therapy (where the phenomenon was first observed). To maximize the abscopal effects of PTT, combination with immunomodulatory agents such as toll-like receptor agonists (TLRs) [9,19] and/or immunotherapies such as checkpoint inhibitors serves as an attractive avenue to potentiate the systemic antitumor immune responses induced by PTT. Several reports have demonstrated the efficacy of combining nanoparticle-based PTT with checkpoint inhibitors to potentiate an abscopal and antitumor immune response mainly in 4T1 breast

* Corresponding author at: The George Washington Cancer Center, The George Washington University, 800 22nd St NW, Science and Engineering Hall, Suite 8410, Washington, DC 20052, USA.
E-mail address: rfernandes@gwu.edu. (R. Fernandes).

http://dx.doi.org/10.1016/j.tranon.2020.100823
1936-5233/©2020 The Authors. Published by Elsevier Inc. on behalf of Neoplasia Press, Inc. This is an open access article under the CC BY-NC-ND license (http://creativecommons.org/licenses/by-nc-nd/4.0/).

cancer models or B16F10 melanoma models. The checkpoint inhibitor aCTLA-4 has been combined with iron-oxide nanoparticles [20], single walled carbon nanotubes [5], and Prussian blue nanoparticles [7]; and the checkpoint inhibitor aPD-1/aPDL-1 has been combined with gold nanostars [21], gold nanorods [22], hollow gold nanoshells [23,24], iron oxide nanoparticles [12], iron oxide-perfluoropentane nanoparticles [25], black phosphorous quantum dots [26], and graphene oxide [27] for PTT. These studies highlight the efficacy of combining nanoparticle-based PTT with immunotherapies. This is because boosting the abscopal effect rates can substantially improve patient care beyond what is currently achieved by each therapy alone, or standard-of-care therapies. In this context, an emerging objective of PTT treatments is to safely maximize the abscopal effect, whereby local administered PTT causes shrinkage of non-treated, distal tumors outside of the primary tumor treatment zone [15,16]. This is especially important for cancers such as neuroblastoma, where patients present with distal or metastatic disease at initial diagnosis; and to address this need, we have tested our nanoimmunotherapy on a syngeneic Neuro2a mouse model of neuroblastoma [28–30].

In this study, we describe Prussian blue nanoparticles (PBNPs) coated with a molecular adjuvant, CpG oligodeoxynucleotides (CpG-PBNPs) [31], a toll-like receptor 9 agonist that we use for PTT (CpG-PBNP-PTT), in combination with the checkpoint inhibitor anti-CTLA-4 (aCTLA-4) as a nanoimmunotherapy that elicits a robust abscopal effect against neuroblastoma. Compared to other nanoparticles used for PTT described above, PBNPs offer several advantages: They are easily and scalably synthesized from inexpensive starting materials [4,32–34], they exhibit pH-dependent biodegradability mitigating concerns associated with their long-term persistence and toxicity within the body (a property not offered by gold nanostructures) [10], and they are already United States FDA-approved for human oral use to treat radioactive poisoning [35,36]. We have previously shown that when delivered in single-tumor models of neuroblastoma, PTT elicits cytotoxicity [4], immunogenic cell death (ICD) [9,11], and increases the antigenicity and adjuvanticity in the tumor environment by itself, and in combination with toll-like receptor agonists like CpG [9] and immunotherapies such as checkpoint inhibitors (aCTLA-4) [10], leading to better treatment outcomes. While these findings suggest that our nanoimmunotherapies work in single-tumor mouse models, it is unclear if they can generate robust systemic antitumor immunity that are able eradicate multiple or disseminated tumors. Given the propensity for high-risk neuroblastoma to present with metastatic disease at initial diagnosis, here, we seek to test the effects of our nanoimmunotherapy in treating mice with bilateral Neuro2a tumors.

We hypothesize that CpG-PBNP-PTT alters the presence of immunomodulatory receptors and ligands on the treated tumor cells (*i.e.* co-stimulatory, inhibitory, etc.), which primes the tumor microenvironment and generates a more potent abscopal effect in the presence of aCTLA-4 (Fig. 1). To test our hypothesis, we utilize the Neuro2a neuroblastoma cell line for our *in vitro* studies and syngeneic mice bearing bilateral Neuro2a tumors for our *in vivo* studies [28–30]. We locally (i.t) administer CpG-PBNPs for PTT, and systemically (intraperitoneally; i.p.) administer aCTLA-4. First, we test the ability of PTT to alter the surface levels of costimulatory and co-inhibitory markers on Neuro2a cells *in vitro*. Next, we assess the effect of our CpG-PBNP-PTT plus aCTLA-4 nanoimmunotherapy on tumor regression and long-term survival. Finally, we test the ability of long-term surviving mice to reject tumor rechallenge and investigate the effect of depleting specific immune cell subsets (CD4+ T cells, CD8+ T cells, and NK1.1+ cells) on the protective effects of our nanoimmunotherapy. The findings of this study will be the basis for further clinical testing and eventual clinical translation of our novel nanoimmunotherapy for treating patients with neuroblastoma.

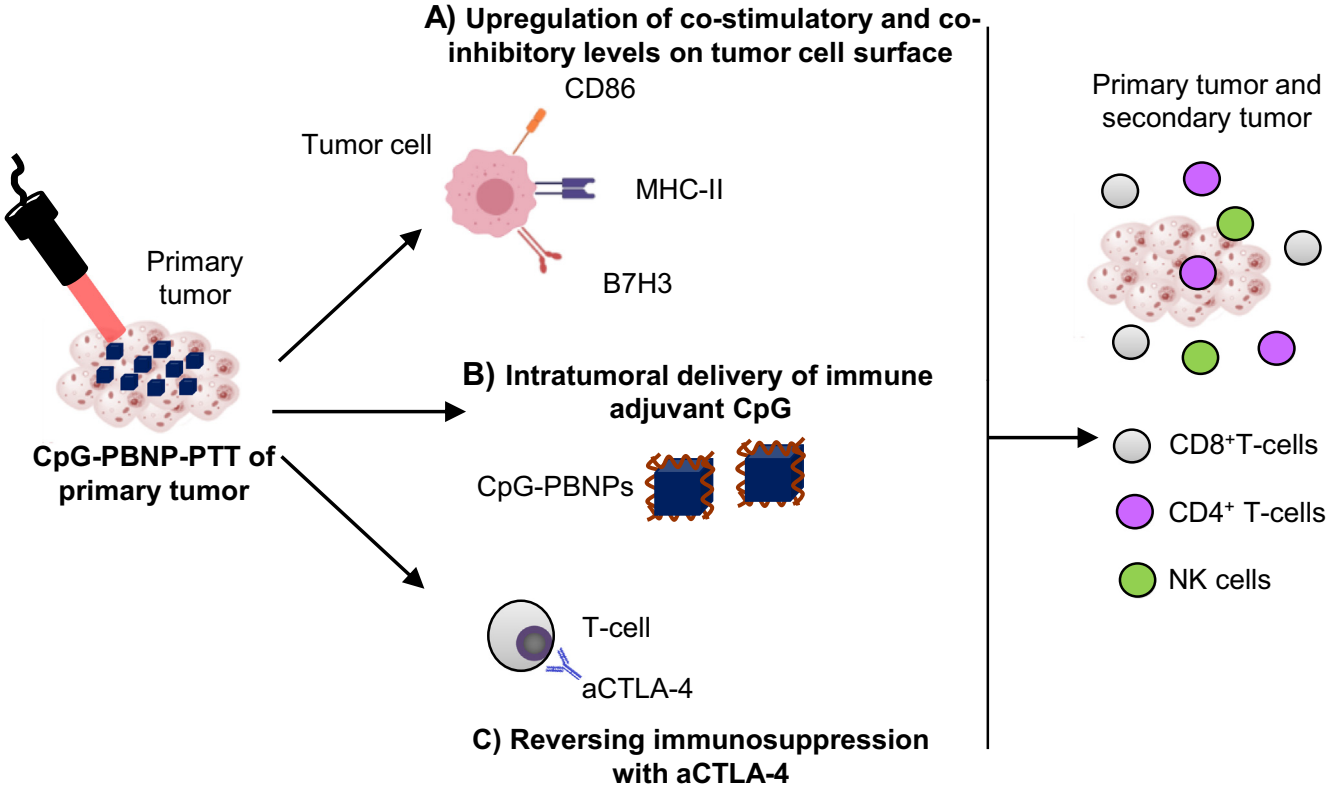

Fig. 1. Nanoimmunotherapy approach combining CpG oligodeoxynucleotide-coated Prussian blue nanoparticle-mediated photothermal therapy (CpG-PBNP-PTT) with anti-CTLA-4 checkpoint inhibition to elicit an abscopal effect against neuroblastoma. CpG-PBNP-PTT (and PBNP-PTT) triggers tumor cell death and alters the (A) cell surface expression of immunomodulatory markers on Neuro2a neuroblastoma tumor cells. (B) CpG-PBNPs facilitates intratumoral delivery of the immune adjuvant CpG, a TLR9 agonist. (C) Systemically administered aCTLA-4 reverses immunosuppression. These three effects function in concert to unleash a robust abscopal effect against neuroblastoma by activating CD4+, CD8+, and NK cells.

Materials and methods

Materials and chemicals

All nanoparticle syntheses were conducted using ultrapure water with a resistivity of 18.2 MΩ cm (Millipore Corporation, Billerica, MA). Potassium hexacyanoferrate(II) trihydrate (MW 422.39; $K_4[Fe(CN)_6]\cdot 3H_2O$), iron (III) chloride hexahydrate (MW 270.3; $Fe(Cl)_3\cdot 6H_2O$), and citric acid were purchased from Sigma-Aldrich (St Louis, MO, USA) and used as supplied. Acetone and ethanol solutions were obtained from Sigma-Aldrich. Poly (ethylenimine) (PEI, Mw 2000, Mn 1800, 50% w/v in H2O) was purchased from Sigma-Aldrich, and diluted in sodium acetate buffer solution (pH 5.2, Millipore Sigma, Burlington, MA). Murine CpG oligodeoxynucleotide (CpG) TLR9 ligand (ODN 1585; Class A) was purchased from InvivoGen

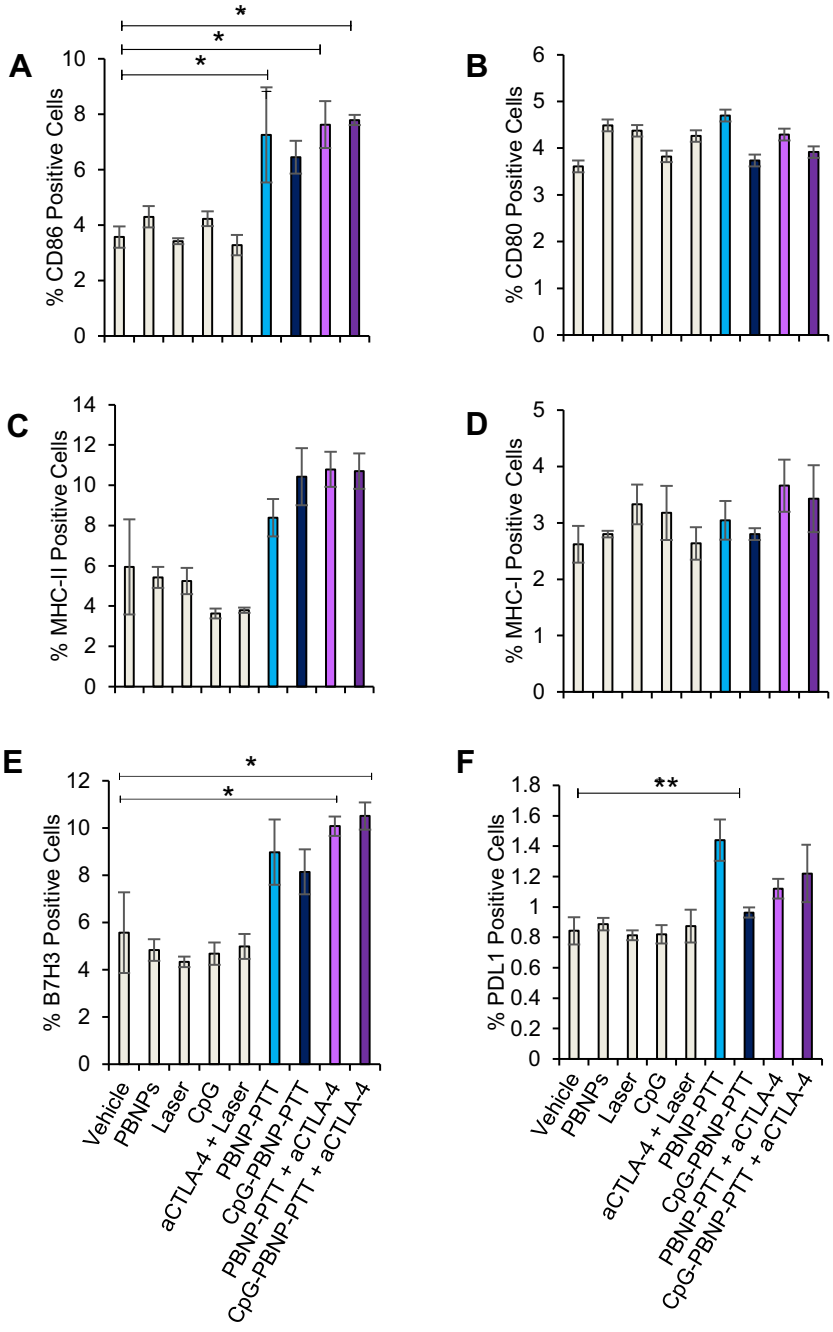

Fig. 2. Effect of PTT on the cell surface levels of immunomodulatory molecules on Neuro2a *in vitro*. (A–B) Co-stimulatory molecule cell surface levels after CpG-PBNP-PTT + aCTLA-4 *in vitro*. Cell surface levels of (A) CD86 and (B) CD80 on Neuro2a cells *in vitro* after CpG-PBNP-PTT + aCTLA-4 and corresponding controls. Cell surface levels were assessed after treatment by flow cytometry. We show a significantly higher percentage of $CD86^+$ cells in cells that were PTT-treated compared to non-PTT-treated. (C-D) Major histocompatibility cell surface levels after CpG-PBNP-PTT + aCTLA-4 *in vitro*. Cell surface levels of (C) MHC-II and (D) MHC-I on Neuro2a cells *in vitro* after CpG-PBNP-PTT + aCTLA-4 and corresponding controls. Neuro2a cells show significantly higher percentage of $MHC\text{-}II^+$ cells in cells that were PTT-treated compared to non-PTT-treated. (E–F) Immune checkpoint molecule cell surface levels after CpG-PBNP-PTT + aCTLA-4 *in vitro*. Cell surface levels of (E) B7H3 and (F) PD-L1on Neuro2a cells *in vitro* after CpG-PBNP-PTT + aCTLA-4 and corresponding controls. Neuro2a cells show significantly higher percentage of $B7H3^+$ cells in cells that were PTT-treated compared to non-PTT-treated (*significant difference compared to vehicle, $p < 0.05$, **significant difference compared to vehicle, $p < 0.01$; $n \geq 3$/group).

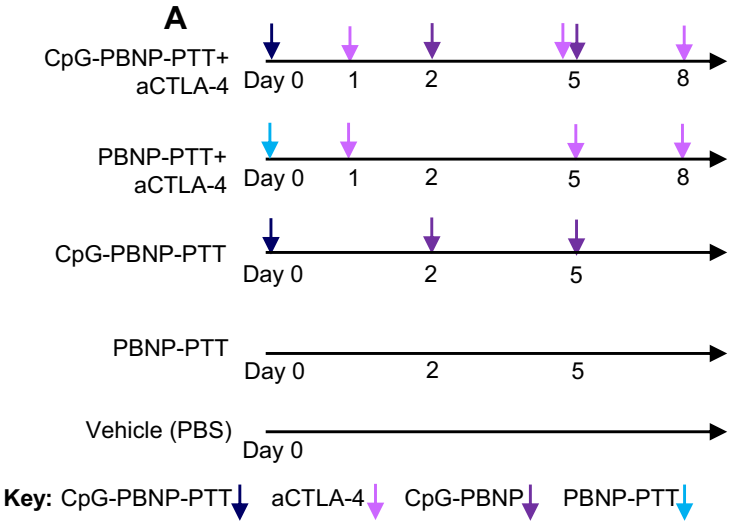

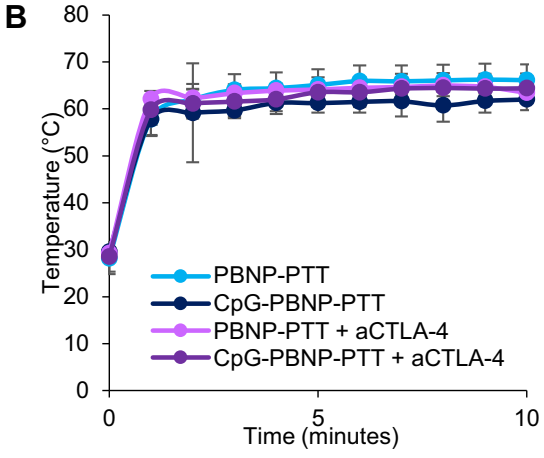

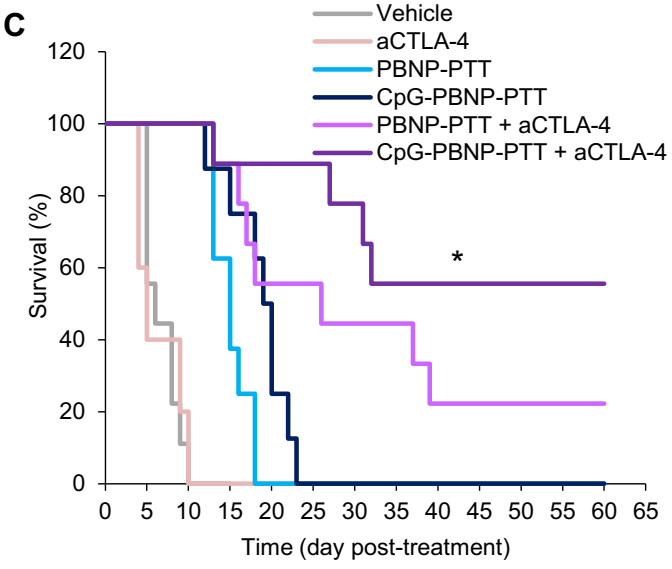

(caption on next page)

(San Diego, CA, USA). Fluorescent antibodies against B7H3, CD276 (B7H3), CD80, CD86, CD274 (B7h1, PD-L1), I-A/I-E (MHC-II), CD45, CD8a, CD4, NK1.1 were purchased from Biolegend (San Diego, CA, USA). Anti-CTLA-4 (aCTLA-4) antibody (clone 9D9) was purchased from BioXCell (West Lebanon, NH), anti-CD4 depletion antibody (clone GK 1.5), anti-CD8 depletion antibody (clone 53–6.7), and anti-NK1.1 (clone PK136) were purchased from Biolegend (San Diego, CA, USA).

Cells and cell culture

The murine neuroblastoma cell line Neuro2a was obtained from American Type Culture Collections (ATCC, Manassas, VA, USA) and cultured in Eagle's Minimum Essential Medium (EMEM) (Gibco, Carlsbad, CA, USA) containing 10% fetal bovine serum (FBS, Gibco) and 1% penicillin/streptomycin (Sigma-Aldrich).

Animals

All animal studies were approved by the Institutional Animal Care and Use Committee of the George Washington University, Washington, DC, USA (Protocol # A396). The studies were conducted to ensure humane care of the animals as per the institutional IACUC guidelines. Five-week-old, female A/J mice were purchased from Jackson Laboratory. The animals were acclimated for 3–4 days prior to tumor inoculation.

Synthesis of PBNPs and CpG-PBNPs

PBNPs were synthesized using a previously described scheme [4,9–11,32–34,37,38]. CpG-PBNPs were synthesized using a layer-by-layer coating methodology previously described by us [9].

In vitro PBNP-PTT and CpG-PBNP-PTT

To study the molecular marker levels after PTT, five million Neuro2a cells were suspended in 500 μL of PBS in a 1.75 mL microcentrifuge tube. Neuro2a cells were divided into eight groups: (1) vehicle (no treatment, 10 μL Milli-Q water), (2) Laser (irradiated at 0.75 W for 10 min), (3) PBNPs (0.15 mg/mL), (4) CpG (40 μg/mL), (5) PBNP-PTT (PBNPs at 0.15 mg/mL, irradiated at 0.75 W for 10 min), (6) CpG-PBNP-PTT (CpG-PBNPs at 0.15 mg/mL, irradiated at 0.75 W for 10 min), (7) PBNP-PTT + aCTLA-4 (PBNPs at 0.15 mg/mL, irradiated at 0.75 W for 10 min, aCTLA-4 at 20 μg/mL) (8) CpG-PBNP-PTT + aCTLA-4 (CpG-PBNPs at 0.15 mg/mL, irradiated at 0.75 W for 10 min, aCTLA-4 at 20 μg/mL). Power was confirmed by a power meter (Thorlabs, Newton, NJ). Temporal temperature measurements were taken using a thermal camera (FLIR, Arlington, VA).

Molecular marker analysis

In vitro CpG-PBNP-PTT + aCTLA-4 and controls were performed as described above. Cell suspensions were then washed and stained with fluorescent antibodies against B7H3, CD276 (B7H3), CD80, CD86, CD274 (B7h1, PD-L1), I-A/I-E (MHC-II), and flow cytometry was performed. Flow cytometry was done using the Celesta Cell Analyzer with HTS (BD BioSciences, Franklin Lakes, NJ), and analysis was done using FlowJo™ software (Ashland, OR).

In vivo studies

For establishing the syngeneic synchronous neuroblastoma mouse model, bilateral subcutaneous injections of one million Neuro2a cells (ATCC) were conducted into the shaved backs of 5-week old female A/J mice. All the treatments commenced after one of the tumors reached a diameter of at least 5 mm ($\sim$60 mm^3). To test the abscopal effect and immune responses of our therapy, synchronous tumor-bearing mice were treated with PTT on the largest tumor (with our nanoparticle-based therapy), and the tumor regression or progression of both tumors was observed. Mice were anesthetized prior to and during treatment using 5% isoflurane. Tumor-bearing mice were divided into five groups ($n \geq 8$ mice per group): (1) vehicle (no treatment, injected intratumorally with 50 μL PBS on day 0), (2) aCTLA-4 (150 μg per mouse administered i.p. on days 1, 4, and 7), (3) PBNP-PTT (50 μL of 1 mg mL^{-1} PBNPs intratumorally, irradiated at 0.75 W for 10 min), (4) CpG-PBNP-PTT nanoimmunotherapy (50 μL of 1 mg mL^{-1} CpG-PBNPs, 2 μg bound CpG, irradiated at 0.75 W for 10 min, CpG-PBNPs boosts were given (without PTT) on days 2 and 5). (5) PBNP-PTT + aCTLA-4 (PBNP-PTT as described above as well as 150 μg aCTLA-4 i.p, on days 0, 3, and 6), and (6) CpG-PBNP-PTT + aCTLA-4 (CpG-PBNP-PTT as described above as well as 150 μg aCTLA-4 i.p on days 0, 3, and 6). The temperatures reached during PTT were measured using an i7 FLIR thermal imaging camera. Tumor growth was monitored following inoculation and treatments using routine caliper measurements. Surviving mice were rechallenged 65 days after treatment with one million Neuro2a cells as described above to assess if the surviving animals developed protection against tumor rechallenge. Animals reached an endpoint if tumor burden exceeded specific dimensions (>15 mm for mice with one tumor, and >13 mm for mice with two tumors. Euthanasia was achieved through cervical dislocation after CO_2 narcosis. All these steps were conducted in accordance with the approved IACUC protocols.

In vivo T cell depletion study

CD8 + T cells, CD4 + T cells, and NK1.1 + cells were depleted by i.p administration of purified anti-CD8α (100 μg/mouse), anti-CD4 (100 μg/mouse), and anti-NK1.1 (100 μg/mouse) depletion antibodies starting a day prior to Neuro2a inoculation and repeating injections on days 3, 6 and 9 after inoculation. Depletion of CD8 + T cells, CD4 + T cells, and NKcells were validated by collecting peripheral blood and analyzing by flow cytometry.

Statistical analysis

Statistical significance was determined from a two-tailed Student's *t*-test and values with $p < 0.05$ qualified as statistically significant. Survival results were analyzed according to a Kaplan-Meier curve. The log-rank test was used to determine statistically significant differences in survival between the various groups.

Results

PTT-containing treatments modulate the cell surface presence of co-stimulatory, antigen-presenting, and immune checkpoint molecules in Neuro2a cells

We have previously demonstrated that PTT using PBNPs (which has a photothermal conversion efficiency of 20.5% [4]), and/or CpG-PBNPs

← **Fig. 3.** Effect of the CpG-PBNP-based nanoimmunotherapy on tumor regression and long-term survival in the synchronous Neuro2a neuroblastoma mouse model. (A) Overview of the treatments. Mice bearing ~5 mm diameter Neuro2a neuroblastoma tumors were treated with CpG-PBNP-PTT + aCTLA-4 and corresponding controls. The PTT-treated groups received 50 μL of 1 mg/mL CpG-PBNPs or PBNPs intratumorally (i.t.), and were irradiated by an 808 nm laser at 0.75 W for 10 min. Additionally, the CpG-PBNP-PTT received two boosters with CpG-PBNP on Days 2 and 5 i.t. The groups that received aCTLA-4 got 150 μg of antibody on days 1, 5, and 8 intraperitoneally (i.p.) (B) Temperature-time profiles of Neuro2a bearing mice treated i.t. with 1 mg/mL CpG-PBNPs or PBNPs and irradiated with a NIR laser at 0.75 W for 10 min. (C) Kaplan-Meier survival plots of neuroblastoma tumor-bearing mice that were treated with PBNP-PTT, CpG-PBNP-PTT, PBNP-PTT + aCTLA-4, CpG-PBNP-PTT + aCTLA-4, or vehicle. Mice receiving CpG-PBNP-PTT + aCTLA-4 showed significantly higher long-term survival (>100 days) compared with mice in the other groups (* significant difference compared to all other groups, $p < 0.05$, long-rank test, $n = 5–9$/group).

leads to tumor cytotoxicity [4,9,10,38], induces immunogenic cell death [9,11], and reverses immunosuppression [9–11,39]. Less well described is the effect of PTT on the surface presence of co-stimulatory, antigen-presenting, and immune checkpoint markers on tumors cells themselves. To this end, we tested the effect of PTT on molecular marker levels on Neuro2a cells, since a robust abscopal effect is likely co-defined by changes to the tumor cells themselves. Therefore, we studied the levels of different co-stimulatory, antigen-presentation, and immune checkpoint markers in Neuro2a cells after nanoimmunotherapy treatments *in vitro* (using flow cytometry). Cells were divided into the following treatment groups: (1) vehicle, (2) laser, (3) PBNPs, (4) CpG, (5) PBNP-PTT, (6) CpG-PBNP-PTT, (7) PBNP-PTT + aCTLA-4, (8) CpG-PBNP-PTT + aCTLA-4. Neuro2a cells exhibited an increase of almost 2-fold in the co-stimulatory molecule CD86 in all PTT treatments compared to controls (Fig. 2A and Supplementary Table 1), while CD80 levels remained the same across all treatment groups (Fig. 2B and Supplementary Table 1). Similarly, we measured the levels of major histocompatibility class I (MHC-I) and II (MHC-II) on the tumor cells. We observed that while MHC-II levels increased across all PTT-treatment groups (Fig. 2C and Supplementary Table 1), MHC-I levels remained the same in all groups compared to controls (Fig. 2D and Supplementary Table 1). Finally, we studied the cell surface presence of immune checkpoint molecules B7-H3 and PD-L1 on Neuro2a cells, and found that even though PTT-treated groups did not increase the presence of PD-L1 (Fig. 2F and Supplementary Table 1), it did increase the presence of B7-H3 (Fig. 2E and Supplementary Table 1). These results demonstrate that in addition to causing tumor cell death, PTT triggers the upregulation of both immunostimulatory and immunosuppressive molecules on Neuro2a cells. These observations provide a rationale for including immunological adjuvants (such as CpG) as well as immune checkpoint inhibitors (such as aCTLA-4) in our nanoimmunotherapy regimen to minimize the suppressive effects of PTT and maximize its abscopal effect.

CpG-PBNP-PTT plus aCTLA-4 nanoimmunotherapy results in tumor regression of treated tumor and an abscopal effect that reduces or eliminates distal tumors

To evaluate the tumor regression and abscopal effects of our nanoimmunotherapy, we utilized a bilateral (two tumor) mouse model. In this model, mice used in the study had two synchronous and subcutaneous Neuro2a tumors. One tumor, designated as the "primary" tumor, was treated with CpG-PBNP-PTT (or controls), and the "secondary" tumor received no treatment. Based on the treatment groups, animals received aCTLA-4, i.p. Tumor progression or regression was measured in all tumors across all five treatment groups (Fig. 3A): 1) CpG-PBNP-PTT + aCTLA-4-treated, 2) PBNP-PTT + aCTLA-4-treated, 3) CpG-PBNP-PTT-treated, 4) PBNP-PTT-treated, 5) aCTLA-4-treated and 6) Vehicle (PBS) ($n \geq 5$/group). PTT was administered at a temperature of approximately 65 °C (average tumor temperature; measured by a thermal imaging camera), which we have previously demonstrated to be the ideal thermal dose to elicit effective tumor ablation as well as immunogenic cell death (ICD) in single Neuro2a tumors (Fig. 3B). Both PBNP-PTT and CpG-PBNP-PTT result in an abscopal effect, as demonstrated by slower tumor growth rates of the secondary tumors compared to vehicle (Fig. 4). These results indicate that local stimulation through PTT confers systemic effects, seen on the secondary tumor. Our nanoimmunotherapy resulted in significant tumor regression and slower tumor growth of the distal tumors compared with vehicle-treated mice. Remarkably, mice treated with CpG-PBNP-PTT + aCTLA-4 resulted in complete tumor regression of both primary and secondary tumors (Figs. 3C and 4), and long-term survival in 55.5% of the treated mice (at 60 days post-treatment, Fig. 3C). The long-term tumor-free survival was significantly higher (55.5% survival) than that observed (at 60 days post-treatment) for mice treated with PBNP-PTT + aCTLA-4 (22.2% survival), CpG-PBNP-PTT (0% survival), PBNP-PTT (0% survival), and vehicle (0% survival). These data demonstrate the importance of all three components: localized PTT, the nanoparticle-localized CpG, and aCTLA-4 to elicit a robust abscopal effect in neuroblastoma.

Long-term surviving, nanoimmunotherapy-treated mice exhibit protection against tumor rechallenge, which is co-defined by CD4+ and CD8+ T cells as well as NK cells

To test whether our nanoimmunotherapy yielded durable responses in treated animals, we challenged long-term surviving nanoimmunotherapy-treated mice with Neuro2a tumor cells (10^6 Neuro2a cells) 65 days post-treatment. Animals were divided into the following groups: 1) naïve group: where untreated mice were challenged with 10^6 Neuro2a cells ($n = 5$), 2) PBNP-PTT + aCTLA-4 rechallenged group: where long-term surviving mice previously treated with PBNP-PTT + aCTLA-4 were rechallenged with 10^6 Neuro2a cells after at least 90 days of tumor-free survival ($n = 2$), and 3) CpG-PBNP-PTT + aCTLA-4: where long-term surviving mice previously treated with CpG- PBNP-PTT + aCTLA-4 were rechallenged with 10^6 Neuro2a cells after at least 65 days of tumor-free survival ($n = 5$). Impressively, all of the rechallenged mice (both PBNP-PTT + aCTLA-4 -treated, and CpG-PBNP-PTT + aCTLA-4 -treated) exhibited protection against the tumor rechallenge, and these mice rapidly eliminated the rechallenged tumors (Fig. 5A), compared with naïve mice that quickly succumbed to their disease by day 7. These results show the ability of our nanoimmunotherapy to treat both primary and secondary tumors as well as confer durable protection to combat recurring disease. In order to understand which immune effector cells were involved in eradicating the tumors following our nanoimmunotherapy, we depleted subsets of T cells by systemic administration of depleting antibodies against CD4+ T cells, CD8+ T cells, and NK cells. The effectiveness of the depletion was confirmed using flow cytometry (Supplementary Fig. 1). When mice that were depleted in CD4+, CD8+, and NK1.1+ populations were treated with our nanoimmunotherapy, they rapidly succumbed to tumor burden, leading to 0% survival at 5, 4, and 9 days after treatment, respectively (Fig. 5B). Tracking the individual tumor growth curves across treatment groups (Fig. 5C–H), we observed that when mice were depleted of $CD4^+$ or $CD8^+$ T cells, CpG-PBNP-PTT offers no tumor burden relief in the primary tumors (Fig. 5C, D), consistent with our previously published data. Since these T cells are crucial for antitumor abscopal effects, the secondary tumors are not killed by a T cell mediated killing, and quickly grow (Fig. 5F–G). When studying the impact of NK cells, we can see that even though NK-depleted mice only survived for two days longer than the T cell-depleted mice, the primary tumor growth for these mice (Fig. 5E) is much slower than those that were depleted of $CD4^+$ and $CD8^+$ T cells. These results highlight the importance of $CD4^+$ and $CD8^+$ T cells as well as NK cells in eliciting antitumor and abscopal responses in synchronous neuroblastoma-bearing mice.

Discussion

In this study, we have described a nanoimmunotherapy, which combines CpG-PBNP-PTT with aCTLA-4 checkpoint inhibition (Fig. 1) for treating neuroblastoma. Building on our previous studies demonstrating PTT eliciting ICD [11], and working synergistically with aCTLA-4 and CpG in single tumor models [9,10], we tested the effect of our nanoimmunotherapy in a synchronous mode of neuroblastoma. Our *in vitro* data (Fig. 2) demonstrated the ability of PTT to modify molecular markers presented on Neuro2a cells suggests their potential, for immune modulation that begins with the tumor cells themselves that are then complemented with immunological adjuvants like CpG and immunotherapies like aCTLA-4 that function on cells of the immune compartment (*e.g.* DCs and T cells). These findings complement earlier published studies by our group that show that PBNP-based PTT also causes cytotoxicity, induction of ICD, and reverse immunosuppression [4,9–11]. We first looked at the presence of co-stimulatory markers CD80 and CD86, and observed that PTT increased the levels of CD86 compared to controls, rendering the tumor cells more immunogenic for triggering the CD28 receptor on T cells. When we studied the presence of major histocompatibility complexes I and II (MHC-I/II), PTT did not increase MHC-I, which helps regulate the sensitivity to antitumoral immunological mechanisms by modifying the

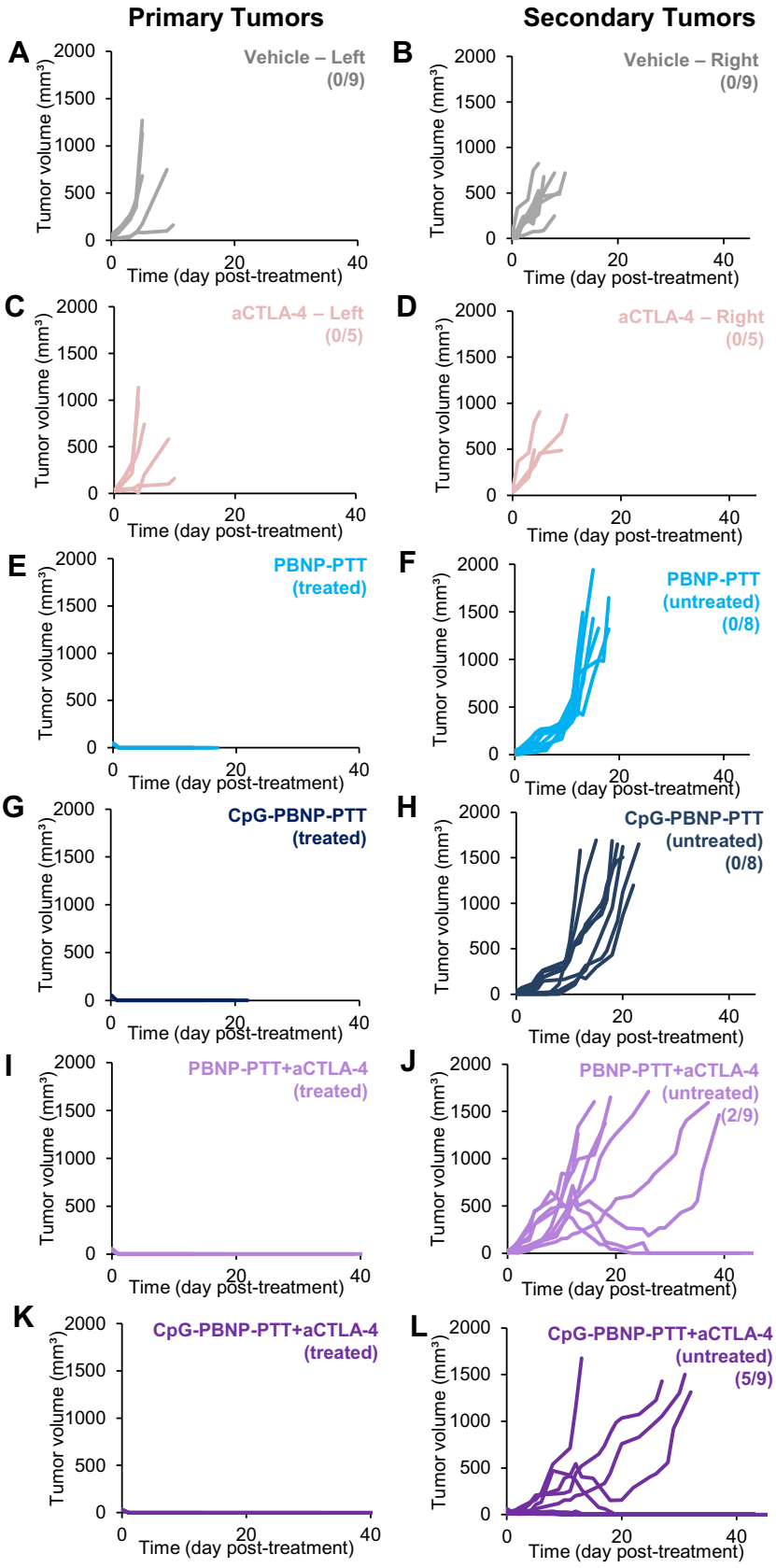

Fig. 4. Effect of the CpG-PBNP-based nanoimmunotherapy on primary and secondary tumor growth in the synchronous Neuro2a neuroblastoma mouse model. Tumor growth in (A–B) vehicle, (C–D) aCTLA-4, (E–F) PBNP-PTT, (G-H) CpG-PBNP-PTT, (I–J) PBNP-PTT + aCTLA-4, and (K–L) CpG-PBNP-PTT + aCTLA-4 treatment groups. Each line represents tumor growth measured in one mouse. Treated/untreated in panels E–L refer to the tumor that received PBNP-PTT treatment. Numbers in parentheses in panels B, D, F, H, J, and L indicate the number of long-term surviving mice in each treatment group *i.e.* greater than 60 day survival (same study as Fig. 3, n = 5–9/group).

recognition of these tumor cells by components of the immune system. However, it increased MHC-II, which is usually found on APCs, but recent studies have shown that on tumor cells, MHC-II levels predicts responses to immune checkpoint blockade, such as aPD-1 [40]. MHC-II levels has also been linked to greater $CD4^+$ T cell infiltrates and some $CD8^+$ T cell infiltrates, which can interact with the activated DCs and aCTLA-4 for better treatments [41–43]. Furthermore, MHC-II presence on tumor cells can also improve endogenous antigen presentation, which induces tumor-specific immunity [44]. Finally, we looked at immune checkpoint molecules, and saw that PTT increases the surface levels of B7H3, but not PD-L1. Both of these checkpoint molecules have inhibitory roles on T cells, leading to tumor evasion [45,46]. However, since B7H3 has immunosuppressive functions, the overexpression of these markers was great motivation for combining our CpG-PBN-PTT with aCTLA-4 for reversal of immune evasion [45–47]. Because molecular marker expression can differ from one tumor type to another, our PTT can be combined with other checkpoint inhibitors as well, such as aPD-1. Additional studies will need to be conducted to address toxicity concerns of the checkpoint inhibitors in clinical trials. Overall, we show that PBNP-based PTT, with and without local CpG and systemic aCTLA-4, can "prime" the tumors for recognition by immune effector cells, an important characteristic for effective combination therapies.

Abscopal effects of PTT are often blocked by the immunosuppressive environment inside the irradiated tumor after treatment, which prevents effective T cell priming [10,18]. In contrast, the combination of immunomodulatory agents such as TLRs and checkpoint inhibitors with PTT can partially reconstitute systemic antitumor immune reactions induced after local tumor PTT. When we studied these effects *in vivo*, CpG-PBNP-PTT in combination with aCTLA-4 resulted in complete tumor

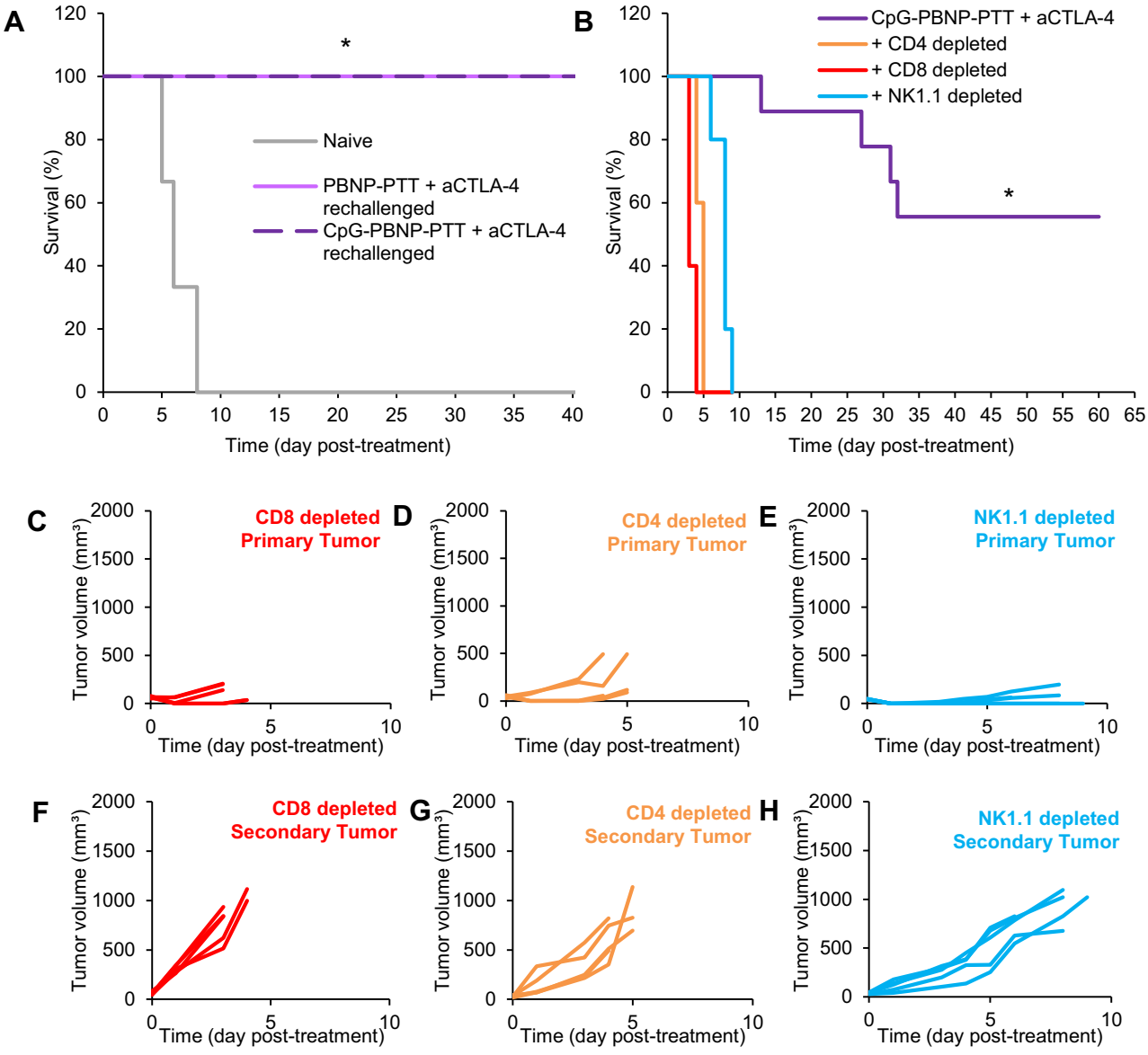

Fig. 5. Effect of tumor rechallenge and immune cell depletion on the protective properties of the nanoimmunotherapy. (A) Effect of rechallenge with 1 million Neuro2a cells in untreated mice (naïve, gray), and long-term surviving nanoimmunotherapies-treated mice; PBNP-PTT + aCTLA-4 (rechallenged, pink), and CpG-PBNP-PTT + aCTLA-4 (rechallenged, purple). The Kaplan-Meier survival plots show complete tumor rejection and significantly higher long-term survival in the rechallenged groups compared to naïve mice (* significant difference compared to naïve mice, $p < 0.05$, $n \geq 3$/group). (B–H) Immune cell depletion show importance of $CD4^+$ and $CD8^+$ T cells on treatment effectiveness. (B) Kaplan-Meier survival plots of neuroblastoma-bearing mice depleted in $CD4^+$ T cells, $CD8^+$ T cells, and $NK1.1^+$ cells. Depletion of these immune cell types ($n = 5$/group) effectively abrogated the therapeutic responses of the nanoimmunotherapy. (C–H) Primary and secondary tumor growth curves for individual mice in the various treatment groups: (C, F) $CD8^+$ T cells depleted, (D, G) $CD4^+$ T cells depleted, (E, H) $NK1.1^+$ depleted. Each line represents tumor growth measured in one mouse. (For interpretation of the references to colour in this figure legend, the reader is referred to the web version of this article.)

regression on the PTT-treated flank, slower progression on the untreated flank, and long-term survival in 55.5% of the synchronous tumor-bearing mice compared to only 22.2% survival in mice treated with PBNP-PTT + aCTLA-4 and 0% survival observed in all mice treated with CpG-PBNP-PTT, PBNP-PTT, aCTLA-4 or left untreated (vehicle) (Figs. 3 and 4). These observations suggest the importance of both intratumoral CpG and systemic aCTLA-4 for a potent abscopal effect.

Long-term surviving mice treated with CpG-PBNP-PTT + aCTLA-4 exhibited protection against tumor rechallenge, indicating the development of immunity and memory responses against these tumors in the mice (Fig. 5). We attribute the significantly higher long-term survival and memory benefit of the nanoimmunotherapy-treated mice to the tumor cell death and priming of the immune response that is elicited by PTT, the improved antigenicity, and DC activation by CpG, and the reversal of T cell exhaustion and immunosuppression by aCTLA-4. Indeed, our studies depleting $CD4^+$ T cells, $CD8^+$ T cells, and $NK1.1^+$ cells populations confirmed the importance of $CD4^+$ and $CD8^+$ T cell populations in complementing and improving the effects of PTT in the local tumor environment, leading to better antitumor systemic and abscopal responses that eliminate distal tumors (Fig. 5). The studies also point to the importance of NK cells, and perhaps other components of innate immunity in providing therapeutic benefits (Fig. 5). Additional studies are necessary to elucidate the underlying immunological mechanisms that elicit these protective responses, and these are the focus of several ongoing studies in our group, including in models of high-risk and metastatic neuroblastoma [48,49]. To summarize, we have demonstrated that engineered nanoparticles can serve as an effective platform for priming and/or activating an antitumor immune response. Hence their use in combination with immunotherapies in nanoimmunotherapies offers possible solutions to overcome the current limitations in cancer immunotherapy. We anticipate that these approaches will be increasingly used for treating cancers with dismal prognoses, including high-risk neuroblastoma, thus extending their benefits to a larger proportion of patients.

Funding sources

This work was supported by the Alex's Lemonade Stand Foundation for Childhood Cancer's 'A' Award, the George Washington University Cancer Center, and the University of Maryland. Research reported in this publication was supported in part by the National Cancer Institute of the National Institutes of Health under Award Number R37CA226171. The content is solely the responsibility of the authors and does not necessarily represent the official views of the National Institutes of Health.

Author contributions

Juliana Cano-Mejia: Conceptualization, Data curation, Formal analysis, Investigation, Methodology, Project administration, Writing – Original draft, Writing – Review & editing Anshi Shukla: Formal analysis, Investigation, Writing – Review & editing Debbie K. Ledezma: Formal analysis, Investigation, Writing – Review & editing Erica Palmer: Investigation, Writing – Review & editing Alejandro Villagra: Resources, Writing – Review & editing Rohan Fernandes: Conceptualization, Data curation, Funding acquisition, Methodology, Project administration, Resources, Writing – Original draft, Writing – Review & editing.

Declaration of competing interest

The authors declare that they have no known competing financial interests or personal relationships that could have appeared to influence the work reported in this paper.

Appendix A. Supplementary data

Supplementary data to this article can be found online at https://doi.org/10.1016/j.tranon.2020.100823.

References

[1] E. Ward, et al., Childhood and adolescent cancer statistics, 2014, CA Cancer J. Clin. 64 (2) (2014) 83–103.
[2] R.L. Siegel, K.D. Miller, A. Jemal, Cancer statistics, 2020, CA Cancer J. Clin. 70 (1) (2020) 7–30.
[3] F. Bellanti, B. Kågedal, O. Della Pasqua, Do pharmacokinetic polymorphisms explain treatment failure in high-risk patients with neuroblastoma? Eur. J. Clin. Pharmacol. 67 (Suppl. 1) (2011) 87–107.
[4] H.A. Hoffman, et al., Prussian blue nanoparticles for laser-induced photothermal therapy of tumors, RSC Adv. 4 (56) (2014) 29729–29734.
[5] C. Wang, et al., Immunological responses triggered by photothermal therapy with carbon nanotubes in combination with anti-CTLA-4 therapy to inhibit cancer metastasis, Adv. Mater. 26 (48) (2014) 8154–8162.
[6] Q. Chen, et al., Photothermal therapy with immune-adjuvant nanoparticles together with checkpoint blockade for effective cancer immunotherapy, Nat. Commun. 7 (2016) 13193.
[7] W. Chen, et al., Combining photothermal therapy and immunotherapy against melanoma by polydopamine-coated Al2O3 nanoparticles, Theranostics 8 (8) (2018) 2229–2241.
[8] L. Guo, et al., Combinatorial photothermal and immuno cancer therapy using chitosan-coated hollow copper sulfide nanoparticles, ACS Nano 8 (6) (2014) 5670–5681.
[9] J. Cano-Mejia, et al., Prussian blue nanoparticle-based antigenicity and adjuvanticity trigger robust antitumor immune responses against neuroblastoma, Biomater Sci 7 (5) (2019) 1875–1887.
[10] J. Cano-Mejia, et al., Prussian blue nanoparticle-based photothermal therapy combined with checkpoint inhibition for photothermal immunotherapy of neuroblastoma, Nanomed. Nanotechnol. Biol. Med. 13 (2) (2017) 771–781.
[11] E.E. Sweeney, J. Cano-Mejia, R. Fernandes, Photothermal therapy generates a thermal window of immunogenic cell death in neuroblastoma, Small 14 (20) (2018), 1800678. .
[12] R. Ge, et al., Photothermal-activatable Fe3O4 superparticle nanodrug carriers with PD-L1 immune checkpoint blockade for anti-metastatic cancer immunotherapy, ACS Appl. Mater. Interfaces 10 (24) (2018) 20342–20355.
[13] A.S. Bear, et al., Elimination of metastatic melanoma using gold nanoshell-enabled photothermal therapy and adoptive T cell transfer, PLoS One 8 (7) (2013), e69073. .
[14] R.H. Mole, Whole body irradiation; radiobiology or medicine? Br. J. Radiol. 26 (305) (1953) 234–241.
[15] M.A. Postow, et al., Immunologic correlates of the abscopal effect in a patient with melanoma, N. Engl. J. Med. 366 (10) (2012) 925–931.
[16] Y. Min, et al., Antigen-capturing nanoparticles improve the abscopal effect and cancer immunotherapy, Nat. Nanotechnol. 12 (9) (2017) 877–882.
[17] J. Abdo, et al., Immunotherapy plus cryotherapy: potential augmented abscopal effect for advanced cancers, Front. Oncol. 8 (2018) 85.
[18] V. Pistoia, et al., Immunosuppressive microenvironment in neuroblastoma, Front. Oncol. 3 (2013) 167.
[19] Q. Han, et al., CpG loaded MoS2 nanosheets as multifunctional agents for photothermal enhanced cancer immunotherapy, Nanoscale 9 (18) (2017) 5927–5934.
[20] H. Chen, et al., Depleting tumor-associated Tregs via nanoparticle-mediated hyperthermia to enhance anti-CTLA-4 immunotherapy, Nanomed. (Lond.) 15 (1) (2020) 77–92.
[21] Y. Liu, et al., Synergistic immuno photothermal nanotherapy (SYMPHONY) for the treatment of unresectable and metastatic cancers, Sci. Rep. 7 (1) (2017) 8606.
[22] B. Zhou, et al., BSA-bioinspired gold nanorods loaded with immunoadjuvant for the treatment of melanoma by combined photothermal therapy and immunotherapy, Nanoscale 10 (46) (2018) 21640–21647.
[23] L. Luo, et al., Sustained release of anti-PD-1 peptide for perdurable immunotherapy together with photothermal ablation against primary and distant tumors, J. Control. Release 278 (2018) 87–99.
[24] L. Luo, et al., Laser immunotherapy in combination with perdurable PD-1 blocking for the treatment of metastatic tumors, ACS Nano 12 (8) (2018) 7647–7662.
[25] N. Zhang, et al., Photothermal therapy mediated by phase-transformation nanoparticles facilitates delivery of anti-PD1 antibody and synergizes with antitumor immunotherapy for melanoma, J. Control. Release 306 (2019) 15–28.
[26] X. Liang, et al., Photothermal cancer immunotherapy by erythrocyte membrane-coated black phosphorus formulation, J. Control. Release 296 (2019) 150–161.
[27] M. Yan, et al., Nanoscale reduced graphene oxide-mediated photothermal therapy together with IDO inhibition and PD-L1 blockade synergistically promote antitumor immunity, ACS Appl. Mater. Interfaces 11 (2) (2019) 1876–1885.
[28] L. Chakrabarti, et al., Reversible adaptive plasticity: a mechanism for neuroblastoma cell heterogeneity and chemo-resistance, Front. Oncol. 2 (2012) 82.
[29] L. Chakrabarti, C. Morgan, A.D. Sandler, Combination of Id2 knockdown whole tumor cells and checkpoint blockade: a potent vaccine strategy in a mouse neuroblastoma model, PLoS One 10 (6) (2015), e0129237. .
[30] L. Chakrabarti, et al., A mechanism linking Id2-TGFbeta crosstalk to reversible adaptive plasticity in neuroblastoma, PLoS One 8 (12) (2013), e83521. .
[31] A.F. Carpentier, et al., Oligodeoxynucleotides containing CpG motifs can induce rejection of a neuroblastoma in mice, Cancer Res. 59 (21) (1999) 5429–5432.
[32] M.F. Dumont, et al., Biofunctionalized gadolinium-containing prussian blue nanoparticles as multimodal molecular imaging agents, Bioconjug. Chem. 25 (1) (2014) 129–137.
[33] M.F. Dumont, et al., Manganese-containing Prussian blue nanoparticles for imaging of pediatric brain tumors, Int. J. Nanomedicine 9 (2014) 2581–2595.
[34] J.M. Vojtech, et al., Biofunctionalized prussian blue nanoparticles for multimodal molecular imaging applications, J. Vis. Exp. 98 (2015), e52621. .
[35] P.J. Faustino, et al., Quantitative determination of cesium binding to ferric hexacyanoferrate: Prussian blue, J. Pharm. Biomed. Anal. 47 (1) (2008) 114–125.

[36] FDA, Radiogardase - Ferric Hexacyanoferrate(ii) Capsule, http://www.accessdata.fda.gov/drugsatfda_docs/label/2008/021626s007lbl.pdf February 9, 2018.
[37] R.A. Burga, et al., Conjugating Prussian blue nanoparticles onto antigen-specific T cells as a combined nanoimmunotherapy, Nanomed. (Lond.) 11 (14) (2016) 1759–1767.
[38] S.S. Kale, et al., Composite iron oxide-Prussian blue nanoparticles for magnetically guided T1-weighted magnetic resonance imaging and photothermal therapy of tumors, Int. J. Nanomedicine 12 (2017) 6413–6424.
[39] E.E. Sweeney, et al., Photothermal therapy improves the efficacy of a MEK inhibitor in neurofibromatosis type 1-associated malignant peripheral nerve sheath tumors, Sci. Rep. 6 (2016) 37035.
[40] D.B. Johnson, et al., Melanoma-specific MHC-II expression represents a tumour-autonomous phenotype and predicts response to anti-PD-1/PD-L1 therapy, Nat. Commun. 7 (2016) 10582.
[41] A. Forero, et al., Expression of the MHC class II pathway in triple-negative breast cancer tumor cells is associated with a good prognosis and infiltrating lymphocytes, Cancer Immunol. Res. 4 (5) (2016) 390–399.
[42] I.A. Park, et al., Expression of the MHC class II in triple-negative breast cancer is associated with tumor-infiltrating lymphocytes and interferon signaling, PLoS One 12 (8) (2017), e0182786. .
[43] L. Mortara, et al., CIITA-induced MHC class II expression in mammary adenocarcinoma leads to a Th1 polarization of the tumor microenvironment, tumor rejection, and specific antitumor memory, Clin. Cancer Res. 12 (11 Pt 1) (2006) 3435–3443.
[44] T.D. Armstrong, et al., Major histocompatibility complex class II-transfected tumor cells present endogenous antigen and are potent inducers of tumor-specific immunity, Proc. Natl. Acad. Sci. U. S. A. 94 (13) (1997) 6886–6891.
[45] J.R. Castellanos, et al., B7-H3 role in the immune landscape of cancer, Am. J. Clin. Exp. Immunol. 6 (4) (2017) 66–75.
[46] Y. Wu, et al., PD-L1 distribution and perspective for cancer immunotherapy-blockade, knockdown, or inhibition, Front. Immunol. 10 (2019) 2022.
[47] A. Ribas, J.D. Wolchok, Cancer immunotherapy using checkpoint blockade, Science 359 (6382) (2018) 1350–1355.
[48] K.J. Ornell, J.M. Coburn, Developing preclinical models of neuroblastoma: driving therapeutic testing, BMC Biomed. Eng. 1 (2019) 33.
[49] A. Kamili, et al., Mouse models of high-risk neuroblastoma, Cancer Metastasis Rev. 39 (1) (2020) 261–274.